Nonlinear Analysis of the Poisson's Ratio of Negative Poisson's Ratio Foams

J. B. CHOI* AND R. S. LAKES**
Center for Laser Science and Engineering
University of Iowa
Iowa City, IA 52242

(Received August 30, 1993)
(Revised February 20, 1994)

ABSTRACT: This article contains an analytic study of Poisson's ratio of re-entrant foam materials with negative Poisson's ratio. These materials get fatter when stretched and thinner when compressed. The Poisson effect is so fundamentally important to the properties of a material that a large change in the value of the ratio will have significant effects on the material's mechanical performance. Isotropic foam structures with negative Poisson's ratio have been fabricated through a permanent volumetric transformation. The cells were converted from the convex polyhedral shape of conventional foam cells to a concave or "re-entrant" shape. Mechanical behavior of a re-entrant open cell foam material will differ from that of a conventional foam in ways not addressed by existing theoretical treatment. Poisson's ratio as a function of strain is obtained by modeling the three-dimensional unit cell as an idealized polyhedron unit cell. Poisson's ratio is predicted to approach the isotropic limit of -1 with increasing permanent volumetric compression ratio of idealized cells, in comparison with experimental values as small as -0.8.

1. INTRODUCTION

CELLULAR MATERIALS ARE multiphase composite material systems that consist of a solid matrix and a fluid phase, the fluid usually being a gas. The matrix makes up an interconnected network of solid struts (ribs) or plates which form the edges and faces of cells. Recently, man has begun to realize the potential of these materials and these cellular solids are increasingly used for structural uses, for insulation, for load bearing, for absorbing the kinetic energy from impact, and as a lightweight core in sandwich panels.

Cellular materials that occur naturally as well as those produced by man have a convex cell shape and exhibit a positive value in Poisson's ratio, which is defined as the negative of the lateral strain divided by the longitudinal strain when a load is applied in the longitudinal direction. In other words, stretching will

[redacted] ** U. WISCONSIN

Reprinted from *Journal of* COMPOSITE MATERIALS, *Vol. 29, No. 1/1995*

cause a decrease in cross-sectional area and compression causes an increase in cross-sectional area. The theoretical allowable range of Poisson's ratio for isotropic material in three dimensions is -1 to 0.5 as demonstrated by energy arguments [1]. An isotropic material with negative Poisson's ratio, however, was not believed to exist until recently. Some anisotropic materials were found to give a negative Poisson's ratio in some directions [2–4].

Recently, isotropic foam structures with negative Poisson's ratio have been fabricated by one of the authors [5]. The fabrication was achieved through a transformation of the cell structure from a convex polyhedral shape to a concave or "re-entrant" shape. The foam ribs can be made of any material; there is no restriction on the chemistry. Negative Poisson's ratio foams have thus far been made of polymers and metals.

The applications of negative Poisson's ratio materials may be envisaged in relation to the Poisson's ratio itself or in relation to other material properties that arise from the unusual structure. In view of Poisson's ratio ν itself, an increase in some material properties such as flexural rigidity, indentation resistance and plane strain fracture toughness was predicted [5–7]. For isotropic material, material properties that depend upon terms such as $(1 - \nu^2)^{-1}$ or $(1 + \nu)$ can attain extremal values as ν approaches -1. Plane strain fracture toughness is one of the material properties that belongs to this category. A possible physical mechanism for the enhancement of this property is that generated internal reactions in structural elements due to negative Poisson's ratio will act to resist crack propagation.

As one of other possible improvements of material properties, a decrease of shear effect in Timoshenko beam with a transverse load is expected. This interpretation is based on Cowper's result [8] for a shear factor k which is a measure of the shear stress distribution in the beam cross section. Cowper has shown a listing of k as a function of Poisson's ratio for several cross sections of beams. The shear factors for any cross section decrease as ν approaches -1 and the effect is most obvious in case of the thin walled tube. This benefit is partly due to the increased shear modulus [9] when Poisson's ratio is negative. Figure 1 shows the difference in the shear effect under a bending deformation of conventional and re-entrant rectangular beam made of Scott industrial foam (Foamade Industries, Auburn Hills, Michigan) which was used in prior experiments [5,9]. The white lines drawn on the surface of the deformed re-entrant beam are more oblique to the horizontal line than those of the deformed conventional beam under the same amount of bending deformation. Consequently, bending deformation rather than shear deformation is dominant in the re-entrant beam because of the negative Poisson's ratio.

So, to summarize, materials with negative Poisson's ratio present a new direction for improving mechanical performance. It is important to understand interactions within the material structure that give rise to negative Poisson's ratio, and it is also necessary to know the global behavior of these novel materials. In this study, the Poisson's ratio of re-entrant foams is obtained by modeling a three-dimensional open cell as an idealized polyhedron unit cell approximating the shape of cells. Experimental results are compared with the modeling.

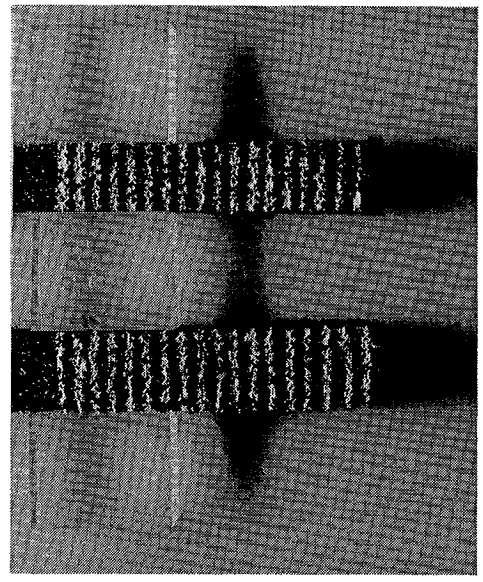

(a)

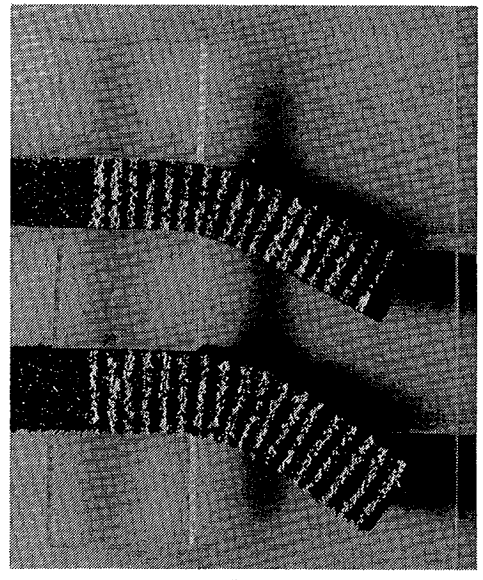

(b)

Figure 1. *Shear effect in the rectangular beams made of Scott foam under a bending mation: (a) natural state; (b) deformed state; in each picture, upper beam, conve foam; lower beam, re-entrant foam.*

2. IDEALIZED UNIT CELL

During foam manufacture, isolated spherical bubbles of gas expand, and as adjacent bubbles come into contact in producing a low density foam, a polyhedral morphology is developed. In the mathematical analyses of the foam material, the real structures have been simulated by the following idealized shapes: sphere [10], cube [11–13], pentagonal dodecahedron [14,15], and tetrakaidecahedron [16–19]. According to Harding's scheme [20], foam cell structures are modeled with a dodecahedron of 12 faces based on the effect of the resultant capillary pressure drop during foam processing. However, the geometrical parameters of a regular tetrakaidecahedron of 14 faces are more susceptible to the formation of an ideal foam structure than a dodecahedron, since a regular tetrakaidecahedron is closer to the geometry of a regular sphere than a regular dodecahedron [21]. Also, Gibson and Ashby [22] showed that many foam cell structures have an average 14 faces and an average 5.1 sides per face. The equivalent polyhedral cell is a tetrakaidecahedron having 6 square and 8 hexagonal faces. Thus, in this study, a regular tetrakaidecahedron is assumed as the mechanical model of the cells of conventional open cell foam materials for the purpose of analysis. The cell model used in this study is shown in Figure 2. The Scott foam used in the experiments was observed to have a similar cell structure (Figure 3).

In experiments with polymer foams [9] and copper foam [23], the re-entrant foam was obtained by applying permanent volumetric compressive deformation with an equal amount in three orthogonal directions. The ratio of initial volume V_i to final volume V_f is the permanent volumetric compression ratio, a processing variable. Three different types of re-entrant cell models can be devised from the conventional unit cell model. In all of them, a rib between two hexagonal faces

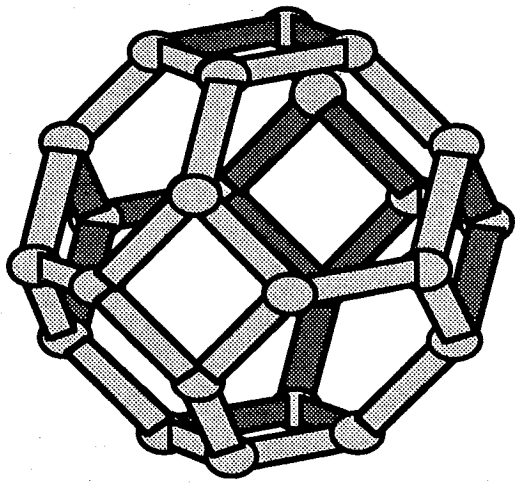

Figure 2. *Idealized conventional unit cell: a regular tetrakaidecahedron.*

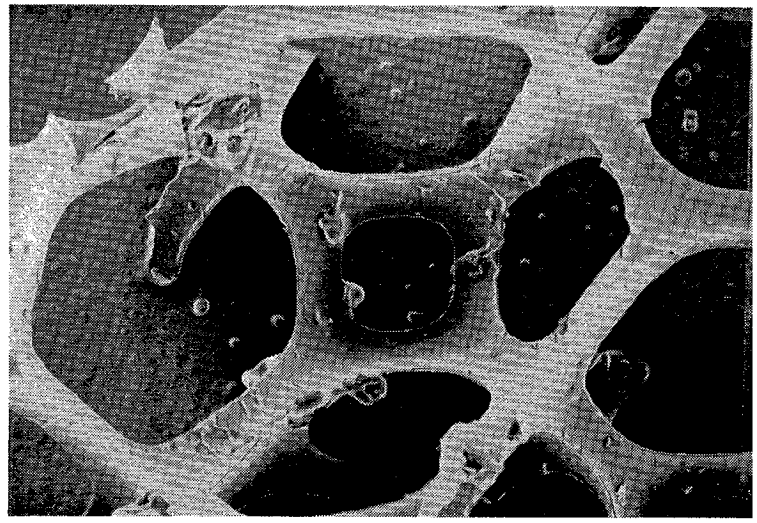

Figure 3. *Scanning electron micrograph of the unit cell of Scott foam which takes the of tetrakaidekahedron.*

is considered to be bent or kinked. In the first type, the bent ribs protrud ward; in the second type, they protrude inward; and in the third hybrid some protrude out and some protrude in. The model with outward protr ribs gives the most negative effect in Poisson's ratio, which is demonstrat simple proof tests using each physical re-entrant unit cell model. Thus, i study, the open cell re-entrant structure is modeled as a re-entrant polyh whose square faces protrude inward at the center position of the cell ribs co ing the square faces, as shown in Figure 4. Figure 5(a) shows a regularly p structure with re-entrant unit cells made of poster board. The length of eac rib is 10 mm. The negativeness in Poisson's ratio of this structure is demons by a simple tension and compression test as shown in the figure. Compress the model gives rise to lateral contraction [Figure 5(b)]. Tension on the gives rise to lateral expansion [Figure 5(c)] as a result of unfolding of the

Because of the symmetry of the conventional and re-entrant models, structures can be analyzed in 2 dimensions to predict their behaviors; Fig shows these two-dimensional cross-sectional views of conventional an entrant cells, which are cut in the diagonal direction of the square face. I figure, A is the cell of the conventional foam. The angle φ will determi volume of the cell and the volumetric compression ratio at each instant. B sents the cell shape at $\varphi = \pi/4$ and C shows one of the re-entrant cell stru when φ is greater than $\pi/4$ and less than $\pi/2$. Cell D indicates the fully pressed state at $\varphi = \pi/2$, resulting in the contact of the adjacent cell ribs. the length change of cell ribs can be neglected without loss of generalit volume V of each cell is expressed by the following equations:

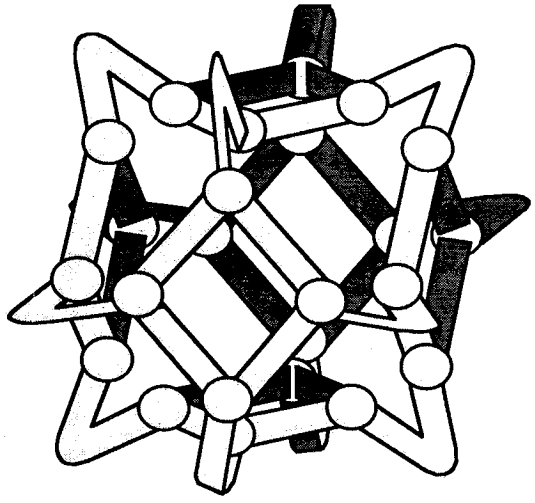

Figure 4. *Idealized re-entrant unit cell.*

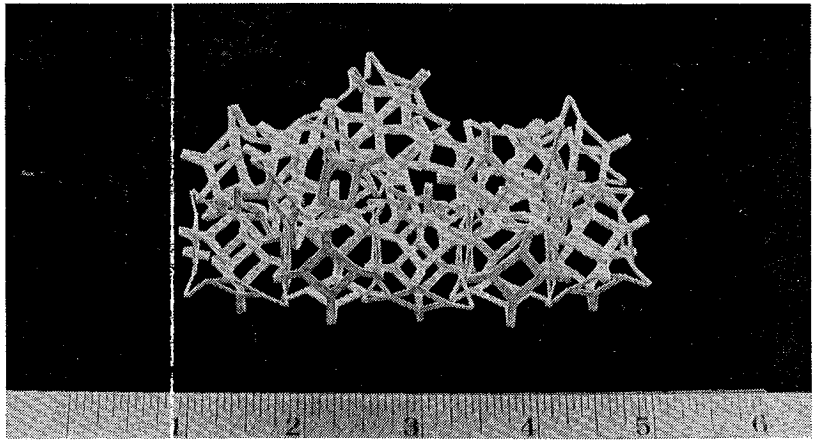

(a)

Figure 5. *A regularly packed structure with idealized re-entrant unit cells made of a poster board and simple tests which shows a negative Poisson's ratio: (a) natural state; (b) compression; (c) tension.*

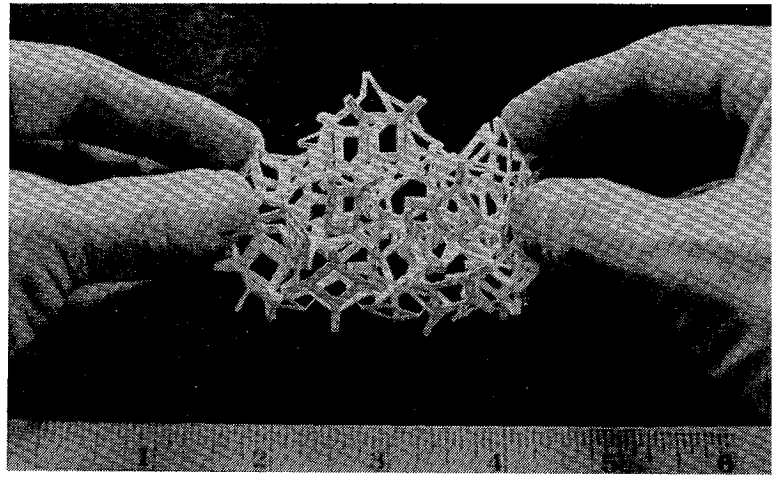

(b)

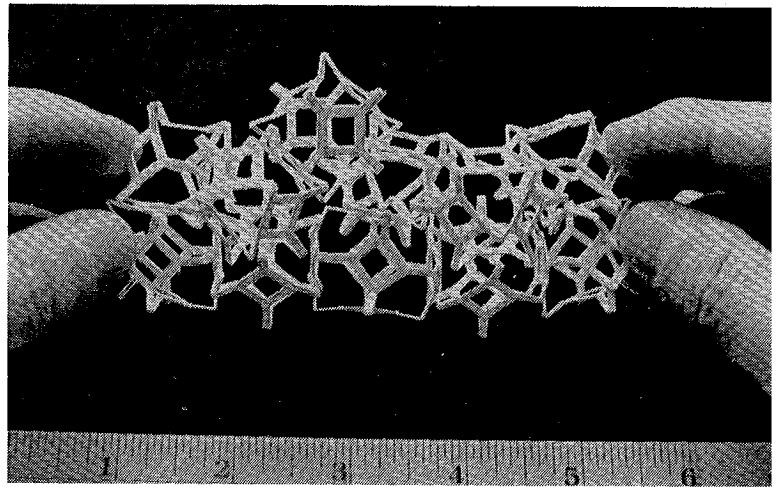

(c)

Figure 5 (continued). *A regularly packed structure with idealized re-entrant unit cells of a poster board and simple tests which shows a negative Poisson's ratio: (a) natural (b) compression; (c) tension.*

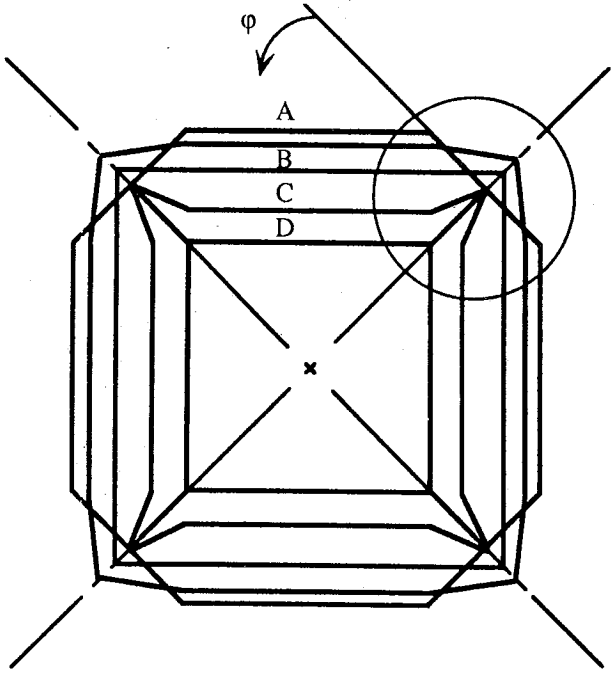

Figure 6. *Two-dimensional cross-sectional view of the idealized conventional and re-entrant unit cell.*

$$V = \frac{1}{2}\tan(\varphi - \pi/4)[\{\sqrt{2} + \cos(\varphi - \pi/4)\}^3 - 2\sqrt{2}]l^3$$

$$+ \frac{45}{8}\sqrt{2}\,l^3,\ 0 \le \varphi \le \frac{\pi}{4} \quad (1$$

$$V = \frac{5}{6}[\sqrt{2} + \sin(\pi/2 - \varphi)]^3 l^3,\ \frac{\pi}{4} \le \varphi \le \frac{\pi}{2} \quad (1$$

where l is the length of the cell rib. Equation (1) is derived by adding the extrud volume from the cube which is enclosed by the convex conventional model. T volumes of the concave re-entrant models [Equation (2)] are obtained by su tracting the intruded volume of the same cube. The volume V_i of a tetrakaidec hedral cell of the conventional foam is $8\sqrt{2}l^3$. Thus, the volumetric compressi ratio is expressed as

$$\frac{V_i}{V_f} = \frac{48}{5}\sqrt{2}[\sqrt{2} + \sin(\pi/2 - \varphi)]^{-3} \quad (1$$

where V_f is the final volume of re-entrant cells. Since each unit cell has 36 ri and every three cells has one rib in common, the relative density ϱ_c/ϱ_s, where is the density of the conventional foam and ϱ_s is the density of the solid, can expressed as $\varrho_c/\varrho_s = 1.06(t/l)^2$, where t is the width of the rib under the assum tion of square cross section. This relation agrees with Gibson and Ashby's resu [22].

3. POISSON'S RATIO OF RE-ENTRANT FOAMS

Figure 7 shows the enlarged view of the re-entrant cell in the circular secti

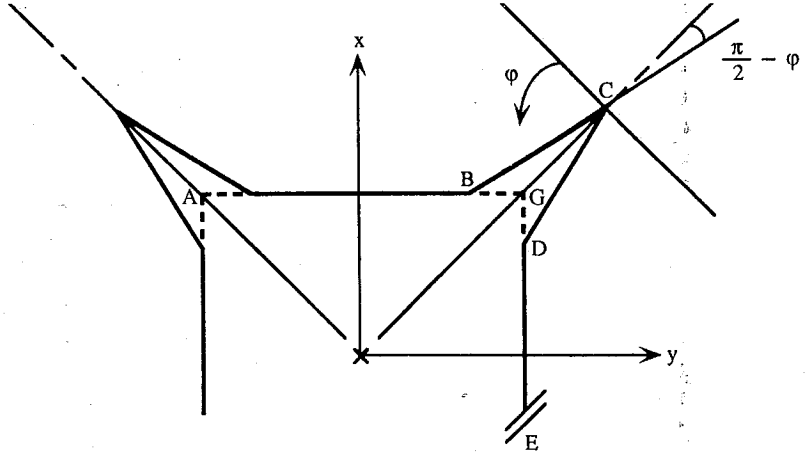

Figure 7. *The enlarged view of the re-entrant cell structure in the circular region in Figure*

in Figure 6. The kinked region is considered to be central to the cell unfolding process responsible for the negative Poisson's ratio. In the case of elastic-plastic material such as copper, the Poisson's ratio of the structure will depend on the elastic bending deformation of cell rib BC at small strain, the rotation of the cell rib around the node C due to plastic hinge formation and the elastic-plastic deformation in the transition region.

A force that is applied at the center of a square face in the regular tetrakaidecahedron produces bending deflections $\delta_x = \delta[\cos(\pi/4) + \cos(\pi/4)]$ and $\delta_y = \delta\cos(\pi/4)$ of the cell ribs. Analysis of these deflections yields a Poisson's ratio of 0.5 for conventional foams at small strain.

Poisson's ratio at small strain will be discussed first. If a force is applied to the square face in the x direction, the cell rib will deflect by an amount of δ, which gives the x component of displacement as $\delta_x = \cos(\varphi - \pi/4)$ and the y component of displacement as $\delta_y = \sin(\varphi - \pi/4)$ from elementary beam theory. The dimension of the cell at a natural state is assumed to be the length AG in Figure 7. Thus, Poisson's ratio ν_{el} at small strain is expressed as follows:

$$\nu_{el} = -\frac{\sin(\varphi - \pi/4)}{\cos(\varphi - \pi/4)} \tag{4}$$

Poisson's ratio ν_{el} at a certain volumetric compression ratio can be determined by Equation (3).

The strains ϵ_x, ϵ_y due to the rotation of cell rib BC around node C are expressed as follows:

$$\epsilon_x = \frac{\sqrt{2}}{2}\frac{\sin(\varphi - \pi/4) - \sin(\varphi - \pi/4 - \theta)}{1 + \sin(\pi/2 - \varphi)}$$
$$\epsilon_y = \frac{\sqrt{2}}{2}\frac{\cos(\varphi - \pi/4 - \theta) - \cos(\varphi - \pi/4)}{1 + \sin(\pi/2 - \varphi)} \tag{5}$$

where θ represents the rotation angle of the cell rib BC in the clockwise direction. Thus, the Poisson's ratio ν_{pl} at large strain after plastic hinge formation is expressed as

$$\nu_{pl} = -\frac{\cos(\varphi - \pi/4 - \theta) - \cos(\varphi - \pi/4)}{\sin(\varphi - \pi/4) - \sin(\varphi - \pi/4 - \theta)} \tag{6}$$

Poisson's ratio ν_{pl} can be related with strain and volumetric compression ratio via Equation (5) and Equation (3), respectively.

Finally, the variation of Poisson's ratio in the transition region during elastic-plastic deformation is calculated. If an applied bending moment in this member BC exceeds the plastic value, an elastic-plastic deformation will occur in the member. A mathematical model applied in this analysis is a built-in cantilever

beam. The deflection at the free end during the elastic-plastic deformation is e pressed as follows under the assumption of a nonhardening material [24]:

$$\frac{\delta}{\delta_e} = \left(\frac{W_e}{W}\right)^2\left[5 - \left(3 + \frac{W}{W_e}\right)\sqrt{3 - \frac{2W}{W_e}}\right] \quad (7)$$

where δ is deflection, W is load, δ_e is deflection at the initial yielding and W_e load at the initial yielding. The plastic boundary is part of a parabola having vertex on the central axis and this boundary grows into the central region of t rib from each side as the deformation continues. The beam eventually collaps when the bending moment at the built-in cross section attains the fully plas value. The collapse load is therefore equal to 1.5 W_e. Since the x component the deflection is $\delta\cos(\varphi - \pi/4)$, the strain ϵ_x becomes

$$\epsilon_x = \epsilon_{ex}\frac{\delta}{\delta_e} \quad (8)$$

where ϵ_{ex} is the x component of strain at the initial yielding. Similarly, from t slope in the deformed beam, the strain ϵ_y is expressed as follows:

$$\epsilon_y = \epsilon_{ey}\frac{\delta}{\delta_e} - \frac{1 - \cos\eta}{2}\epsilon_{ex},\ \eta = \left(\frac{W_e}{W}\right)\left[3 - 2\sqrt{3 - \frac{2W}{W_e}} - \frac{W}{W_e}\right] \quad (9)$$

where ϵ_{ey} is the y component of strain at the initial yielding.

Thus, Poisson's ratio variation ν_{el-pl} upon strain during elastic-plastic deform tion becomes

$$\nu_{el-pl} = \nu_y - \epsilon_{ex}\frac{1 - \cos\eta}{2\epsilon_x} \quad (10)$$

where ν_y is the Poisson's ratio at the initial yielding. The load varies from t initial yielding load W_e to the collapse load 1.5 W_e. At each amount of the loa strain components ϵ_x and ϵ_y can be determined by Equation (8) and Equation (9 respectively. Finally, Poisson's ratio can be related with volumetric compressi ratio by Equation (3). For small strains, we expect $\nu_y \approx \nu_{el}$.

4. DISCUSSION AND COMPARISON WITH EXPERIMENT

Experimental results used for comparison are from previous studies up polymer foams [9] and copper foam [23]. Figure 8 shows the analytical relati of the volume of the cell and volumetric compression ratio to the angle φ. $\varphi = \pi/4$ and $\varphi = \pi/2$ which are the minimum and maximum values for t foam to be re-entrant, volumetric compression ratios are 1.4 and 4.8, respe

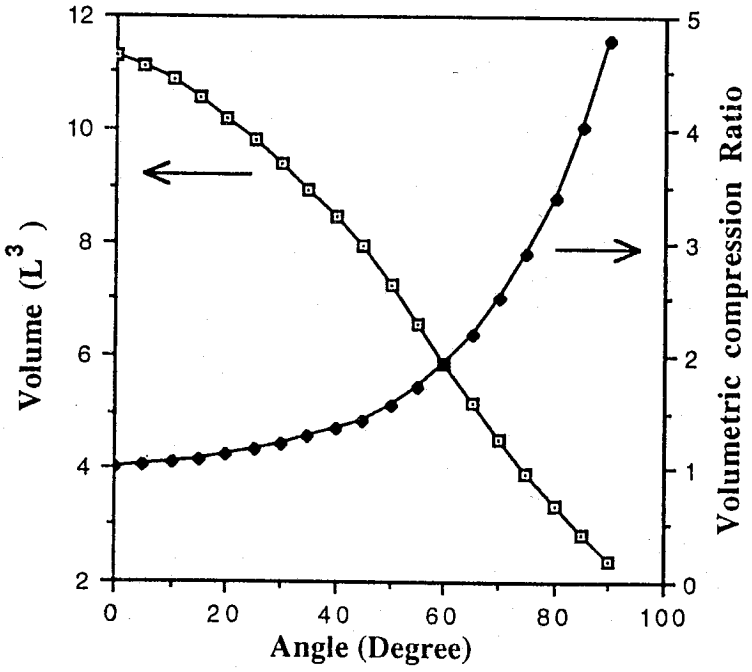

Figure 8. *Volume of the conventional, re-entrant unit cell and volumetric compression ratio vs the angle φ in the cell model.*

tively. Experiment disclosed that negative Poisson's ratio was best produced in the range of volumetric compression of 3.3 to 3.7 because of the recovery and the cell rib adhesion in polymer foams. A re-entrant polymer foam of volumetric compression ratio of 1.6 showed a negative effect in Poisson's ratio. Moreover, foam could not be transformed beyond a volumetric compression ratio of 5.0 because of contact and adhesion of the cell ribs. Thus, the present model is considered to be satisfactory.

Figure 9 shows the minimum Poisson's ratio that a re-entrant foam can have at small strain with a certain volumetric compression ratio. The present analysis is for elastic-plastic foams. Experimental results for polymer foams which are elastomeric foams, are used in the comparison with the modeling result in Figure 9. This was done since a full data set was not available for copper foam. The comparison is meaningful because all kinds of foams have the same deformation mechanism within the linear elastic region at small strain. The experimental results for elastomeric polymer foams show a similar behavior to that predicted by the analysis except at a large volumetric compression ratio at which the re-entrant foam had some cell rib adhesion and contact that diminished the negative effect in Poisson's ratio. The analysis predicts a Poisson's ratio of 0.5 for conventional foam, in agreement with Reference [17]. The reason is that the ribs are

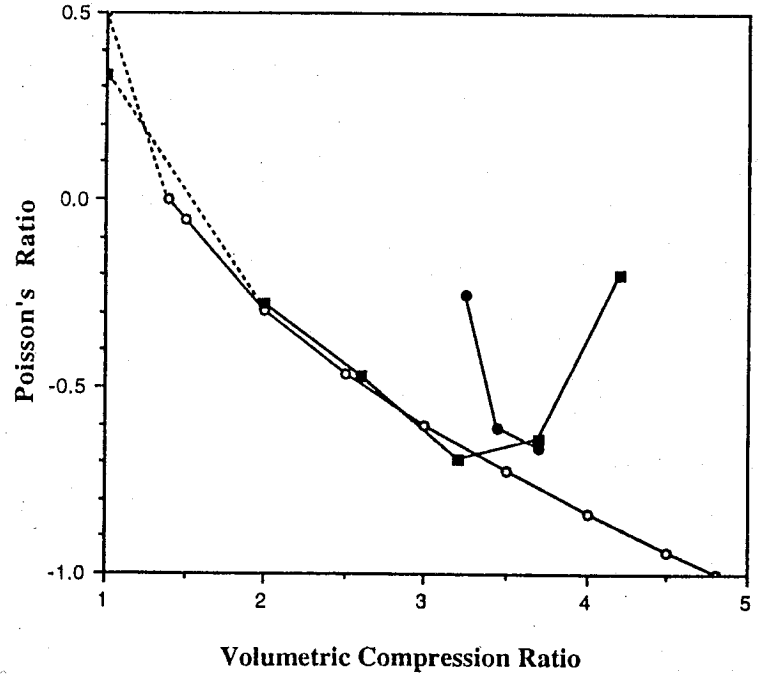

Figure 9. *Minimum Poisson's ratio that a re-entrant foam can have at a certain volumet compression ratio: open symbol, modeling; solid symbols, experiment [9]; open squa Scott foam in tension, strains less than 0.5%; open circle, grey foam in tension, at 5% stra*

assumed to be straight, so that their rigidity in tension/compression, which governs the bulk modulus, greatly exceeds their rigidity in bending, which governs the shear and Young's modulus. In actual foams of conventional structure, there may be some initial curvature or misalignment of the ribs which would give rise to a lower Poisson's ratio approaching 0.3.

Furthermore, actual re-entrant foam structure is more complex and irregular than that assumed in the analysis. It is not composed of only one type of re-entrant unit cell but has a hybrid re-entrant structure. This study used only the re-entrant cell model which gives the best negative effect in Poisson's ratio among the three cell models. Thus, the theory gives a slightly better negative Poisson's ratio than experiment over the whole range of volumetric compression ratio.

Figure 10 shows the comparisons for predicted Poisson's ratio vs strain with the experimental data for copper foam. The strain at the initial yielding, ϵ_{ex}, was assumed as 1% in both volumetric compression ratios of 2.0 and 2.5. Analysis and experiment are in good agreement with each other at a volumetric compression ratio of 2.0. But, at a volumetric compression ratio of 2.5, the shape of the curves is similar, but the magnitudes differ. At a high permanent volumetric compression ratio the cells become more convoluted; moreover there is the possibil-

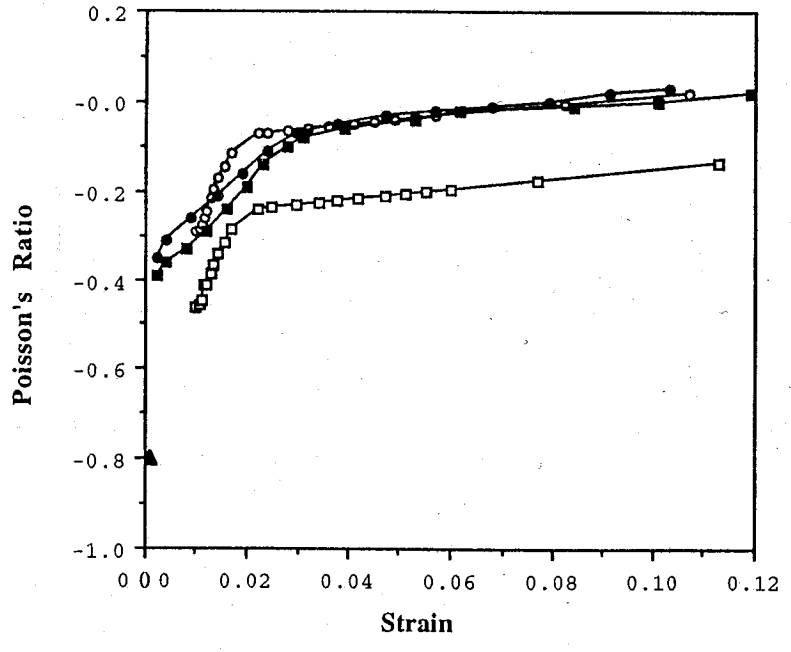

Figure 10. *Comparison of the modeling result to the experimental data for copper foam: open symbols, modeling; solid symbols, experiment [23]; circles, volumetric compression ratio 2.0; squares, volumetric compression ratio 2.5; triangle, optical test result, volumetric compression ratio 2.13.*

ity of non-homogeneous compression, and damage of cell ribs, which could count for the discrepancy. In the calculation of the Poisson's ratio ν_{el-pl} dur elastic-plastic deformation, the Poisson's ratio ν_{el} at small strain was replaced the value of the Poisson's ratio ν_y at the initial yielding. As is obvious from characteristic curve of Poisson's ratio upon strain which includes Poisson's ra of -0.8 obtained by an optical test (Figure 10), the re-entrant foams have a v sharp cusp in Poisson's ratio for strains less than the yield strain. In this rega the ν_y value will differ from the ν_{el} value. And also experimental results for c per foam [23] which is an elasto-plastic foam, showed a change of yield str with volumetric compression ratio. The yield strain was 0.2% offset yield str and actual initial yield strain should be smaller than that. At a permanent vo metric compression ratio of 2.5, the modeling results approach the experimer data if one chooses a smaller value of the initial yield strain and a smaller solute value of Poisson's ratio at the initial yielding. The model in the pres study is confined to Poisson's ratio of elasto-plastic re-entrant foam material o a range of strain. But, all kinds of re-entrant foams made of elastomeric foa elasto-plastic foam and brittle foam, can be described by Equation (4) for value of Poisson's ratio at small strain. The polymer foams used in experime [9] which are nonlinear elastic materials, can be analyzed similarly at large str because they exhibit cell rib rotation similar to the plastic hinge formation of elastic-plastic foam. The Poisson's ratio of the polymer foams had a similar cu behavior with copper foam even if it was much broader (about a factor of 10) th that of copper foam.

Other kinds of negative Poisson's ratio materials have also been repor [25–30]. Since the physical mechanisms for the behavior may differ, neither present analysis nor the observed nonlinearities of re-entrant foams can be pected to apply to all materials with a negative Poisson's ratio. However a cu in the dependence of Poisson's ratio on strain also occurs in negative Poisso ratio cellular solids [27,28] of microstructure quite different from the re-entr foams considered here. The common element appears to be the realignment the geometrical configuration responsible for the negative Poisson's ratio deformation occurs.

5. CONCLUSION

1. The analysis predicts that Poisson's ratio for small strain decreases as the p manent volumetric compression ratio increases. Analysis and experim agree reasonably well down to $\nu = -0.7$.

2. Poisson's ratio of re-entrant foams is dependent upon strain and has a cu shape at relatively small strain. Elastic-plastic deformation of elasto-plas foams gives rise to a sharp cusp.

3. The model in the present study explains Poisson's ratio of elasto-plastic entrant foam material in the regions of linear elasticity, elastic-plastic def mation and plastic collapse.

REFERENCES

1. Fung, Y. C. 1968. *Foundation of Solid Mechanics.* Englewood Cliffs, NJ: Prentice-Hall.
2. Love, A. E. H. 1944. *A Treatise on the Mathematical Theory of Elasticity.* NY: Dover Pub.
3. Miki, M. and Y. Murotsu. 1989. *JSME International Journal,* 32:67–72..
4. Tsai, S. W. and H. T. Hahn. 1980. *Introduction to Composite Materials,* Lancaster, PA: Technomic.
5. Lakes, R. S. 1987. *Science,* 235:1038–1040.
6. Lakes, R. S. 1987. *Science,* 238:551.
7. Friis, E. A., R. S. Lakes and J. B. Park. 1988. *J. Mat. Sci.*, 23:4406–4414.
8. Cowper, G. R. 1966. *J. Appl. Mech.*, (June):335–340.
9. Choi, J. B. and R. S. Lakes. 1992. *J. Mat. Sci.*, 27:4678–4684.
10. Green, D. J. and R. G. Hoagland. 1985. *J. Am. Ceram. Soc.*, 67(7):395–398.
11. Ko, W. L. 1965. *J. Cell. Plast.*, 1:45–50.
12. Gibson, L. J. and M. F. Ashby. 1982. *Proc. R. Soc. Lond.*, A382:43–59.
13. Gent, A. N. and A. G. Thomas. 1963. *Rubber Chem. Technol.*, 36:597–610.
14. Menges, G. and F. Knipschild. 1975. *Polym. Eng. Sci.*, 15(8):623–627.
15. Chan, R. and M. Nakamura. 1969. *J. Cell. Plast.*, 5:112–118.
16. Doherty, D. J., R. Hurd and G. R. Lester. 1962. *Chemistry and Industry,* pp. 1340–1356.
17. Dement'ev, A. G. and O. G. Tarakanov. 1970. *Mekh. Polim.*, 6(5):859–865.
18. Dement'ev, A. G. and O. G. Tarakanov. 1970. *Mekh. Polim.*, 6(4):594–602.
19. Dement'ev, A. G. and O. G. Tarakanov. 1971. *Mekh. Polim.*, 7(4):670–675.
20. Harding, R. H. 1967. *Resinography of Cellular Plastics.* ASTM Publication STP 414.
21. Shutov, F. A. 1983. *Adv. Polym. Sci.*, 51:177–178.
22. Gibson, L. J. and M. F. Ashby. 1988. *Cellular Solids.* Oxford: Pergamon Press.
23. Choi, J. B. and R. S. Lakes. 1992. *J. Mat. Sci.*, 27:5375–5381.
24. Chakrabarty, J. 1987. *Theory of Plasticity.* NY: McGraw-Hill.
25. Almgren, R. F. 1985. *J. Elasticity,* 15:427–430.
26. Herakovich, C. T. 1985. *J. Composite Materials,* 18:447–455.
27. Caddock, B. D. and K. E. Evans. 1989. *J. Phys. D., Appl. Phys.*, 22:1877–1882.
28. Evans, K. E. and B. D. Caddock. 1989. *J. Phys. D., Appl. Phys.*, 22:1883–1887.
29. Haeri, A. Y., D. J. Weidner and J. B. Parise. 1992. *Science,* 257:650–652.
30. Lakes, R. S. 1993. *Advanced Materials,* Weinheim, Germany, 5:293–296.